Clim Dyn (2015) 45:2885–2899
DOI 10.1007/s00382-015-2512-6

Recent surface mass balance from Syowa Station to Dome F, East Antarctica: comparison of field observations, atmospheric reanalyses, and a regional atmospheric climate model

Yetang Wang · Shugui Hou · Weijun Sun · Jan T. M. Lenaerts · Michiel R. van den Broeke · J. M. van Wessem

Received: 5 June 2014 / Accepted: 4 February 2015 / Published online: 13 February 2015

Abstract Stake measurements at 2 km intervals are used to determine the spatial and temporal surface mass balance (SMB) in recent decades along the Japanese Antarctic Research Expedition traverse route from Syowa Station to Dome F. To determine SMB variability at regional scales, this traverse route is divided into four regions, i.e., coastal, lower katabatic, upper katabatic and inland plateau. We also perform a regional evaluation of large scale SMB simulated by the regional atmospheric climate model versions 2.1 and 2.3 (RACMO2.1 and RACMO2.3), and the four more recent global reanalyses. Large-scale spatial variability in the multi-year averaged SMB reveals robust relationships with continentality and surface elevation. In the katabatic regions, SMB variability is also highly associated with surface slope, which in turn is affected by bedrock topography. Stake observation records show large inter-annual variability in SMB, but did not indicate any significant trends over both the last 40 years for the coastal and lower katabatic regions, and the last 20 years record for the upper katabatic and inland plateau regions. The four reanalyses and the regional climate model reproduce the macro-scale spatial pattern well for the multi-year averaged SMB, but fail to capture the mesoscale SMB increase at the distance interval ~300 to ~400 km from Syowa station. Thanks to the updated scheme in the cloud microphysics, RACMO2.3 shows the best spatial agreement with stake measurements over the inland plateau region. ERA-interim, JRA-55 and MERRA exhibit high agreement with the inter-annual variability of observed SMB in the coastal, upper katabatic and inland plateau regions, and moderate agreement in the lower katabatic region, while NCEP2 and RACMO2.1 inter-annual variability shows no significant correlation with the observations for the inland plateau region.

Keywords Surface mass balance · Antarctica · Spatial variability · Temporal variability · Model assessment

Y. Wang (✉) · W. Sun
College of Population, Resources and Environment, Shandong Normal University, Jinan 250014, China
e-mail: wangyetang@163.com

Y. Wang
Shandong Marine Resource and Environment Research Institute, Yantai 264006, China

S. Hou
MOE, Key Laboratory for Coast and Island Development, School of Geographic and Oceanographic Sciences, Nanjing University, Nanjing 210093, China

J. T. M. Lenaerts · M. R. van den Broeke · J. M. van Wessem
Institute for Marine and Atmospheric Research Utrecht, Utrecht University, Utrecht, The Netherlands

1 Introduction

Any mass fluctuation of the Antarctic Ice Sheet may have a large influence on global sea level due to its huge volume, which could raise sea level by 56.6 m if melted (IPCC AR5). Therefore, a considerable effort has been put into the accurate quantification of Antarctic mass balance and its contribution to sea level rise. Common research methods include: the translation of observed surface elevation to mass changes (e.g., Davis et al. 2005; Helsen et al. 2008), satellite gravimetry changes (e.g., Moore and King 2005; Velicogna 2009; Barletta et al. 2013; Sasgen et al. 2013) and input and output calculation, i.e., the difference between ice discharge (e.g., Wingham et al. 2006; Rignot et al. 2011) and surface mass balance (SMB), which is defined as the sum of precipitation of snow, surface sublimation (SU_s), drifting snow sublimation (SU_{ds}), wind-driven erosion/deposition (ER_{ds}), and meltwater runoff. Until now, more than 20 Antarctic mass balance evaluations have been performed on the basis of the satellite techniques of altimetry, interferometry, and gravimetry (Zwally and Giovinetto 2011; Shepherd et al. 2012). However, these estimates from the limited temporal coverage of satellite observation (altimetry: since 1992; gravimetry: since 2003) should be considered with caution because change in SMB over short time periods may be as large as their uncertainties. In addition, recent Antarctic elevation variability revealed by radar altimetry is mainly dependent on snow accumulation changes (Helsen et al. 2008; Ligtenberg et al. 2014). Thus, an accurate SMB assessment is still a key constraint for determining temporal evolution in Antarctic mass balance. Quantifying Antarctic SMB is also vital to correctly interpret ice core records, detect the ice-dynamic response related to climate changes, and to force ice sheet models.

To accurately determine Antarctic SMB, several studies have used interpolation of direct accumulation rates data from ice cores, snow pits and stake measurements (Vaughan et al. 1999; Giovinetto and Zwally 2000; Arthern et al. 2006). However, these lack the temporal resolution and the spatial coverage of field data is limited. Due to the sparse coverage and the short timespan of SMB observations, and high temporal variability of the SMB, a reliable long-term Antarctic SMB dataset is very difficult to build, requiring more field observation and modeling results.

With recent advances in climate model physics and resolution, as well as climate data assimilation and representation, global reanalyses generated by a numerical weather prediction model calibrated with meteorological observations have the potential to accurately simulate Antarctic SMB. In addition, reanalyses have been widely applied to evaluate Polar SMB (e.g., Monaghan et al. 2006a; Burgess et al. 2010; Hanna et al. 2011), and to force regional climate models (e.g., Van de Berg et al. 2006; Lenaerts et al. 2012a, b; Gallée et al. 2013) because they follow the observed climate, where climate models do not. However, the reanalyses and climate models need to be verified using field observations before they could be used to investigate the spatial and temporal variability in Antarctic SMB. Bromwich et al. (2011) made a comparison between SMB from six new reanalyses and spatial accumulation rate estimate based on field observations by Arthern et al. (2006). Agosta et al. (2013) evaluated a downscaled SMB model using an updated compilation of SMB field measurements (Favier et al. 2013). Most recently, several studies assessed the skill of the reanalysis and atmospheric models to determine Antarctic regional snow accumulation over Adelie Land (Agosta et al. 2012), Fimbul ice shelf (Sinisalo et al. 2013) and Thwaites Glacier (Medley et al. 2013). However, more regional evaluation studies are required, especially in the data-sparse East Antarctic inland plateau.

Since the 1950s, glaciological investigations in eastern Dronning Maud Land have been carried out by the Japanese Antarctic Research Expeditions (JAREs) (GSI 2007). As part of these programs, stakes were installed every 2 km along the traverse route from coastal Syowa Station (S16 point) (69°02′S, 40°03′E, 580 m a.s.l.) to Mizuho Station (70°42′36″S, 44°18′54″E, 2230 m a.s.l.) to determine the changes in the ice sheet SMB since 1968. The 32nd and 33rd JAREs in 1991 and 1992 extended the stake measurement at 2 km intervals from Mizuho Station directly toward inland Dome F (77°22′S, 39°42′E, 3810 m a.s.l.). Most of these stakes were measured at least once per year. While some data reports and preliminary results on snow accumulation derived from stake measurements were published (e.g., Fujiwara and Endo 1971; Endo and Fujiwara 1973; Takahashi et al. 1994; Furukawa et al. 1996; Satow et al. 1999; Kameda et al. 2008), there is still much to be done to determine SMB from the coast to the inland plateau of East Antarctica. Therefore, our main objective is to examine the spatial and temporal variability in SMB along the transection from Syowa Station to Dome F, and to evaluate the global reanalysis products and regional climate model output for SMB variability using these field measurements.

2 Data and method

2.1 In situ observation data

Net snow accumulation measurements by stakes along the JARE traverse route from Syowa Station (S16) to Dome F (Fig. 1) were derived from the National Institute of Polar Research archives (JARE data reports), accessed online at http://ci.nii.ac.jp/organ/journal/INT1000001377_en.html. Along this route, 504 bamboo stakes (2.5 m long) anchored 60–90 cm deep in snowpack were used to monitor snow height changes at 2 km intervals. Each stake bottom was fixed on a horizontal slab by means of an anchor. If snowfall during the following year was likely to bury more than the emerging part of a stake, the stake was replaced with a new one, and the replaced one was placed at its original location. A GPS survey measured surface ice movements at 11 sites along this stake-line between 1992 and 2004, and showed that the maximum horizontal velocity was <25 m a^{-1} (Motoyama et al. 2008). To minimize the effect of ice movement on the SMB measurement, once a stake moved away more than 100 m, a replacement stake would be put back in its initial location. Missing stake measurement data make up only six percent of all stake

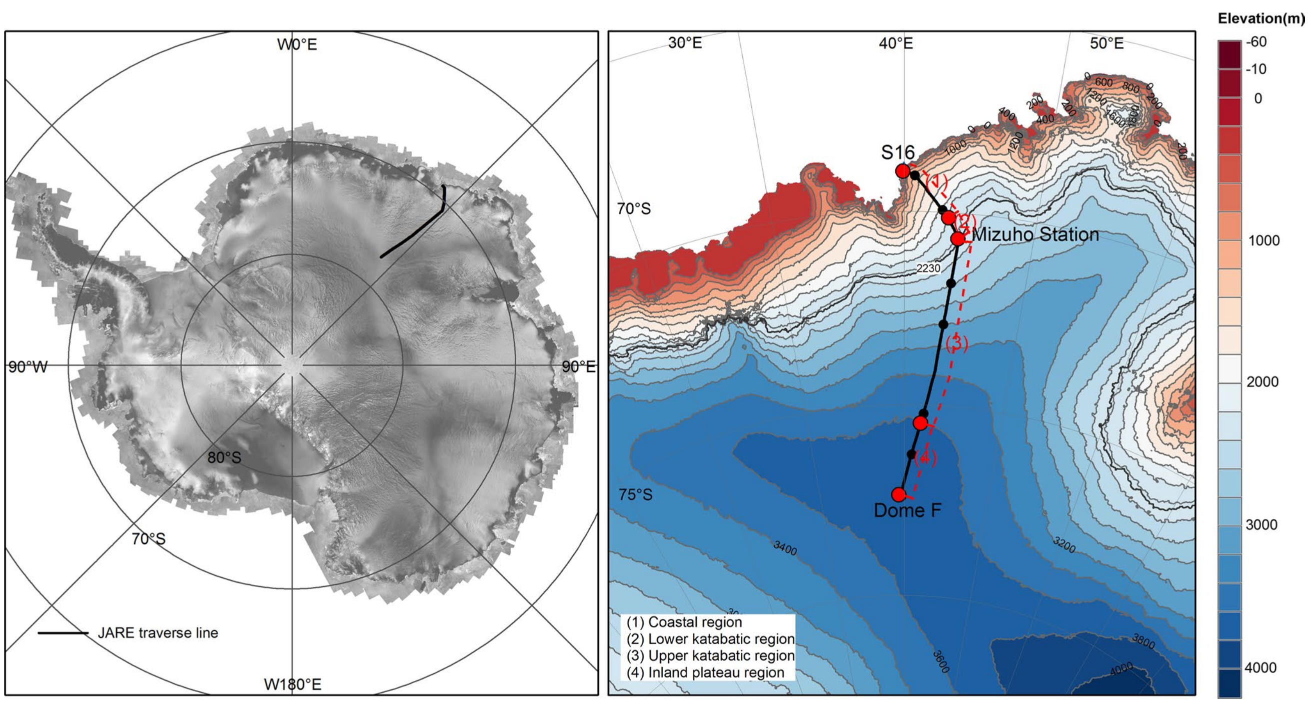

Fig. 1 Location of JARE stake measurements and surface elevation from Bamber et al. (2009)

observations, and are concentrated in the year 1974. Thus, we discarded the 1974 data.

To convert accumulated snow depth to SMB, surface snow density information is a prerequisite. Surface snow density was measured at 10 km intervals (168 sites) along the route between Syowa Station and the inland Plateau Station in 1967–68, which is very close to the JARE traverse route (Fujiwara and Endo 1971). Surface snow density measurements were collected at 112 locations between S16 and Mizuho Station at the same position of stakes during January 1982 by JARE (Ohmae 1984). During the period 1995–97, surface snow densities at 107 sites, where the surface snow conditions seem to be the most typical, were measured along the whole traverse route from S16 to Dome F (Azuma et al. 1997; Motoyama and Fujii 1999). These surface snow densities are averaged values from the upper 10 or 20 cm of snow. The recent observed mean snow density for the upper 1 (or 0.5) m layer at the 21 sites of the traverse route from Syowa station to Dome F were also collected by the Japanese-Swedish Antarctic Expedition 2007/08 (Sugiyama et al. 2012). The error for the snow density measurements was estimated to be ±4 % (Conger and McClung 2009). Despite the large quantity of density measurements, a lot of stake locations still have no density information. To determine SMB for every stake, the snow density values were interpolated using the dependence of surface density on wind speed and surface elevation, described best by a second-order polynomial (Fig. 2), and then smoothed by a 10 km weighed average to remove spatial and measurement noise. These interpolated densities were multiplied by the accumulated depth to convert stake measurements into water-equivalent, and to update the multi-year mean SMB during the period from 1993 to 2010 from Favier et al. (2013).

2.2 Reanalysis and regional climate model data

Four global atmospheric reanalyses and one regional climate model are assessed based on SMB observation. They include the Medium-Range Weather Forecasts ''Interim'' reanalysis (ERA-interim), the Modern-Era Retrospective Analysis for Research and Applications (MERRA), the Japan Meteorological Agency (JMA) 55-year Reanalysis (JRA-55), the Department of Energy Atmospheric Model Intercomparison Project 2 reanalysis (NCEP2), and two version of the regional atmospheric climate model (RACMO2). Table 1 describes their main characteristics. SMB is estimated as precipitation minus surface evaporation/sublimation (P–E) in the global reanalyses. It is calculated as precipitation minus surface and drifting snow sublimation, and wind-driven snow deposition/erosion in the RACMO2.

ERA-interim global atmospheric reanalysis data were obtained from the European Centre for Medium-Range Weather Forecasts (ECMWF). Based on a 4D-VAR

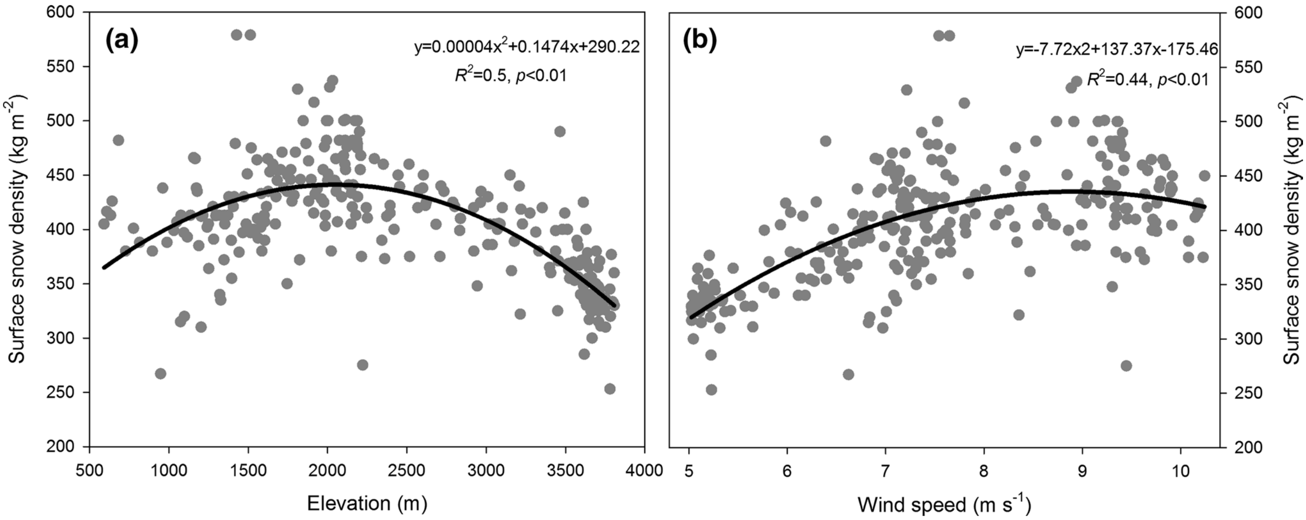

Fig. 2 Snow density averaged from the surface to 20, 50 cm, or 1 m depth versus surface elevation (**a**), and multi-year averaged wind speed (**b**). Density data come from Fujiwara and Endo (1971), Endo and Fujiwara (1973), Naruse (1975), Watanabe (1975), Ohmae (1984), Azuma et al. (1997), Motoyama and Fujii (1999), Kameda et al. (2008), and Sugiyama et al. (2012); Multi-year averaged wind speed (1979–2011) comes from the output of a regional atmospheric climate model (Lenaerts and Van den Broeke 2012)

Table 1 Characteristics of the reanalyses and regional atmospheric climate model used in this study

Reanalysis	Organization	Time coverage	Horizontal resolution	Vertical levels	Assimilation system
NCEP2	NCEP/DOE	1979–present	1.875°; ~210 km	28	3DVAR
JRA-55	JMA/CRIEPI	1955–present	0.5625°; ~60 km	60	4DVAR
ERA-Interim	ECMWF	1979–present	0.703125°; ~80 km	60	4DVAR
MERRA	NASA GMAO	1979–present	0.5° × 0.667°; ~55 km	72	3DVAR
RACMO2	KNMI[a]	1979–2011	0.25°; ~ 27 km	40	–

[a] KNMI/IMAU: Royal Netherlands Meteorological Institute—The Netherlands

assimilation system, ERA-interim is the latest global atmospheric reanalysis with 60 atmospheric vertical levels (Simmons et al. 2009), covering a time period from 1979 to the present. Compared to the 40-year ECMWF Re-Analysis (ERA-40), ERA-interim has a higher resolution (T255, ~0.7° i.e., ~80 km), with substantial improvements in its representation of the hydrological cycle, and temporal consistency on a range of time-scales. This was achieved through better model physics and assimilation system efficiency, as well as the bias correction in satellite radiances and surface pressure observations (Detail description see Dee et al. 2011).

MERRA (Bosilovich et al. 2008; Rienecker et al. 2011) is a second reanalysis produced by NASA's Global Modeling and Assimilation Office. It provides a spatially and temporally continuous record of observational analyses covering the period 1979 to present. The atmospheric model applied in this reanalysis is a three-dimensional variational (3D-VAR) Goddard Earth Observing System Data Assimilation System (GEOS-5) with 72 vertical levels and a horizontal resolution of only 0.5° × 0.667° (nominal resolution of 55 km). MERRA has improved the evaluation of the large-scale hydrological cycle and global precipitation by assimilating Special Sensor Microwave Imager (SSM/I) and the Tropical Rainfall Measuring Mission (TRMM) Microwave Imager (TMI) observations. According to Bosilovich et al. (2008) and Decker et al. (2012), the performance of MERRA for precipitation simulation is close to or better than other reanalyses such as the Climate Forecast System Reanalysis (CFSR) from NCEP, ERA-40 and ERA-interim.

JRA-55 is the first reanalysis extended to 55 years starting from 1958, when the global radiosonde observing system was first set up. This reanalysis is generated based on JMA's operational numerical weather prediction (NWP) system (a 4D-VAR data assimilation system) as of Dec 2009. Improvements in this reanalysis include increased model resolution [JRA-55: nominally 0.5625° (~60 km) and 60 vertical atmospheric levels; JRA-25: nominally 1.125° (~125 km) and 40 vertical atmospheric levels], an

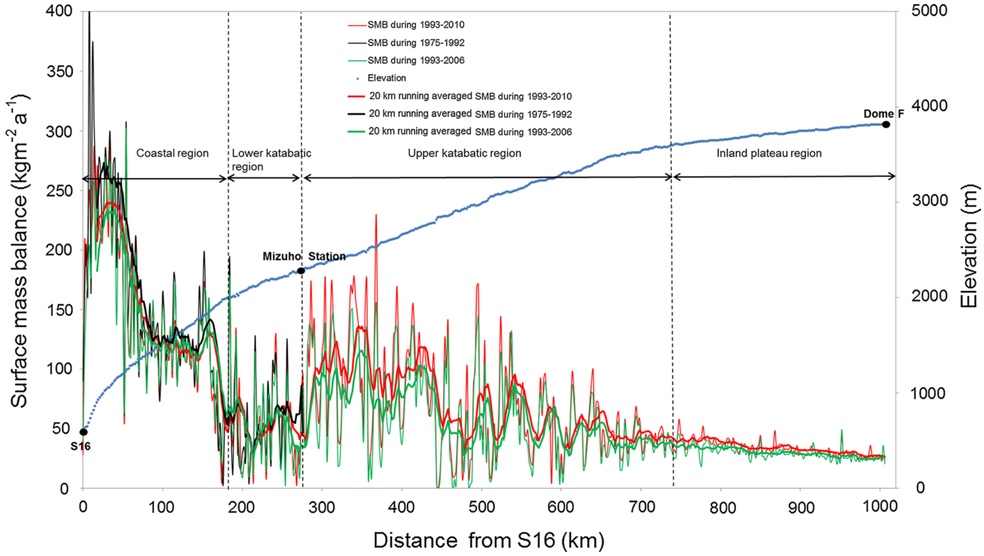

Fig. 3 The spatial distribution of multi-year averaged SMB along JARE traverse route for the different periods

advanced 4D-VAR data assimilation scheme with bias correction for satellite radiances, and updated dynamical and physical processes. As a result, JRA-55 provides a better reanalysis than the Japanese 25-year Reanalysis (JRA-25) (Ebita et al. 2011). Note that JRA-25 precipitation has better correlation with global precipitation analyses than NCEP-2 and ERA-40 (Onogi et al. 2007; Bosilovich et al. 2008), while in turn JRA-55 precipitation shows a higher correlation with global precipitation analyses than that of JRA-25 (Ebita et al. 2011).

NCEP-2 is an updated version of the National Centers for Environmental Prediction–National Center for Atmospheric Research (NCEP–NCAR) reanalysis by utilizing an improved data assimilation system and forecast model with the horizontal resolution of nominally 1.875° (~210 km) and a vertical resolution of 28 levels.

RACMO2 is modified for the use over ice sheets (Ettema et al. 2009), and incorporates the atmospheric dynamics from the High Resolution Limited Area Model (HIRLAM) and physical processes from the ECMWF model. This regional climate model was run including drifting snow physics presented in Lenaerts et al. (2010, 2012a, b), and the lateral boundary conditions are derived from ERA-interim reanalysis (1979–2011). RACMO2 has 40 vertical atmospheric levels and a horizontal resolution of 0.25°, i.e., ~27 km. To further improve the SMB processes, RACMO version 2.1 (RACMO 2.1) was further upgraded to version 2.3 (RACMO2.3) which includes a new parameterization for cloud microphysics, as well as improvements in the cloud, radiation and turbulence parameterizations (Van Wessem et al. 2014). Note that RACMO2 does not assimilate the observations, i.e., the model is allowed to be evolved freely in its interior domain.

3 Results

3.1 Observed spatial variations of SMB along the JARE traverse route

The SMB measurements are first averaged over two time periods, 1975–1992 and 1993–2010, for each of the stake locations along the traverse route from S16 to the Mizuho Station. We then compare the 20-km running average of the two time-averaged SMB data sets, and find a remarkably similar spatial pattern (Fig. 3). This shows that the 18-year (1993–2010) SMB data are representative for the SMB averaged over long time scales. As Fig. 3 shows, the time-averaged SMB (1993–2010) shows great spatial variability, but in general decreases in a fluctuating fashion from the coast S16 to inland Dome F. This general pattern is also observed along other transects from Terra Nova Bay to Dome C (Frezzotti et al. 2005), and from Zhong Shan Station to Dome A (Ding et al. 2011). Figure 3 shows that SMB is high near the coast and decreases inland until ~270 km from S16; it then increases until ~350 km from S16 and decreases again until Dome F.

Following previous studies on regional snow surface features (Fujiwara and Endo 1971; Watanabe 1978; Furukawa et al. 1996), this transection can be divided into three regions, i.e., a coastal region, a katabatic region and an inland plateau region. Given the different time coverage of stake measurements along this traverse route (S16-Mizuho Station: since the 1970s; Mizuho Station-Dome F: since the 1990s), and the opportunity to assess the inter-annual variability of SMB in the reanalysis and regional climate model using these measurements, we further divide the katabatic region into two regions, i.e., a lower katabatic region and an upper katabatic region. The coastal region is defined as the

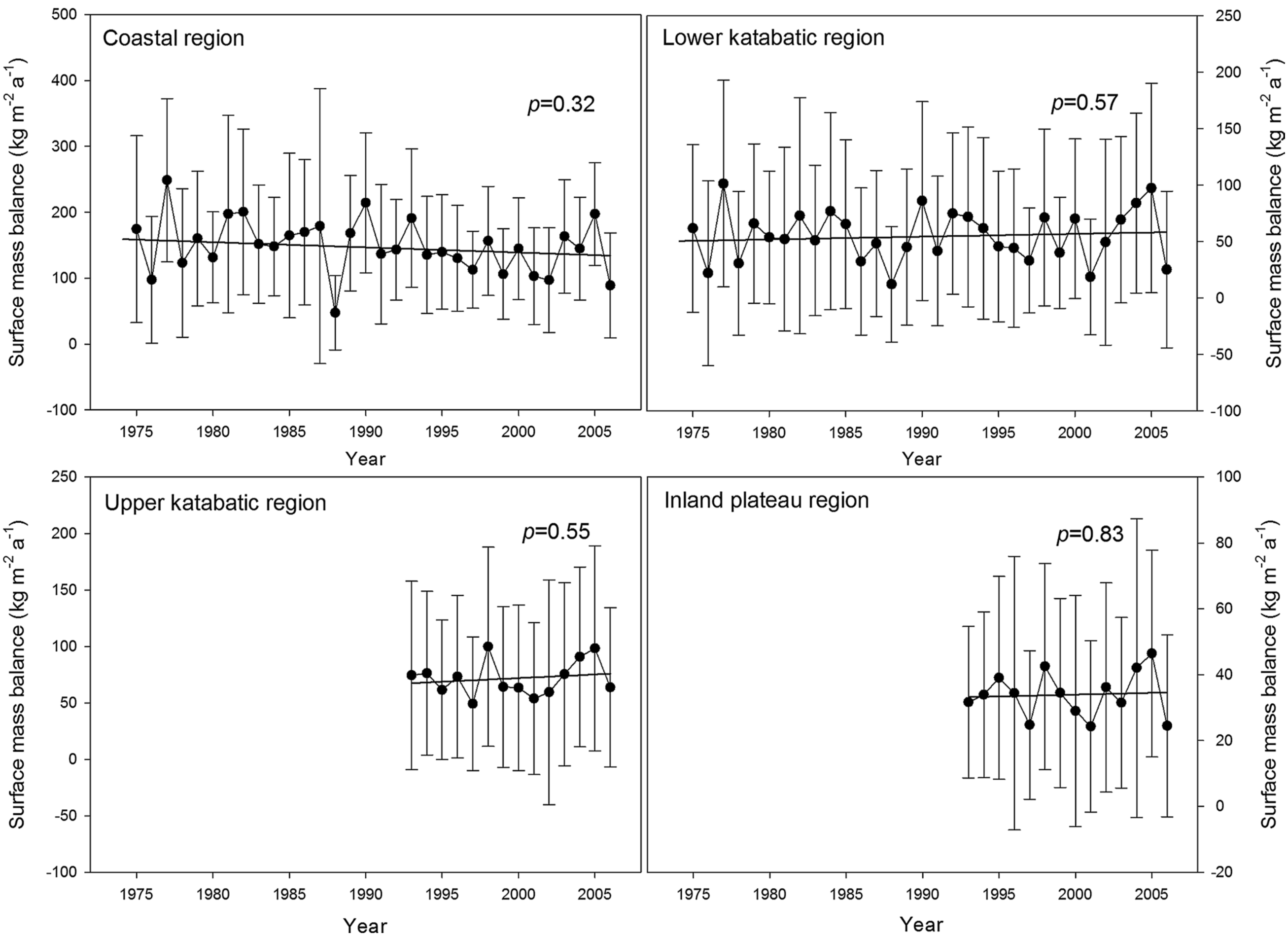

Fig. 4 The inter-annual variability of SMB over coastal region, lower katabatic region, upper katabatic region, and inland plateau region

region below 2000 m in elevation and with <186 km distance from S16, dominated by small sastrugi and dunes. This region is characterized by a sharp decline in SMB from coast towards the interior, which is caused by the decreasing precipitation with increasing elevation, drifting snow and sublimation. The lower katabatic wind region lies between 2000 and 2230 m in elevation and at a distance of 186–258 km from S16. The SMB decreases at the distance interval 186–210 km from S16, and then SMB in a fluctuating fashion increases until 258 km distance from S16. The upper katabatic region lies between 2230 and 3600 m in elevation, and at 258–742 km from S16. Despite the increasing elevation, SMB presents an increasing trend at the distance interval 258–370 km from S16. A significant decline in SMB is found for the distance interval 370–742 km from S16. The inland plateau region is the region above 3600 m elevation, at a distance of 742–1006 km from S16, which is dominated by small sastrugi and dunes. This region has a low averaged SMB of 34 kg m^{-2} a^{-1}, a standard deviation of 15 %, and a relatively low temporal variability (max: 47 kg m^{-2} a^{-1}, min: 6 kg m^{-2} a^{-1}), due to the weak wind.

3.2 Observed temporal variations of SMB along the JARE traverse route

Figure 4 indicates the time series of annual mean SMB and its standard deviation summarized by the four regions along the traverse route between coastal S16 and inland Dome F. As shown by the large error bars (standard deviation), the SMB at individual stakes along this transection shows very large fluctuations. The temporal variability in SMB differs among the four regions. The inter-annual variability in SMB is largest for the coastal and lower katabatic regions: the highest year in this period (1977) had a value 5 times greater than the lowest year (1988). The upper katabatic and inland plateau regions show relatively small inter-annual variability in SMB, with standard deviations of 22 and 21 %, respectively (Fig. 4). The linear regressions of SMB time series show no statistically significant trends for any of the regions. The slope is slightly negative for the coastal region and positive for the lower katabatic region for the time period of 1975–2006. Slightly positive slopes are observed for both the upper katabatic and inland plateau regions for the time period 1993–2006 (Fig. 4). 20 km

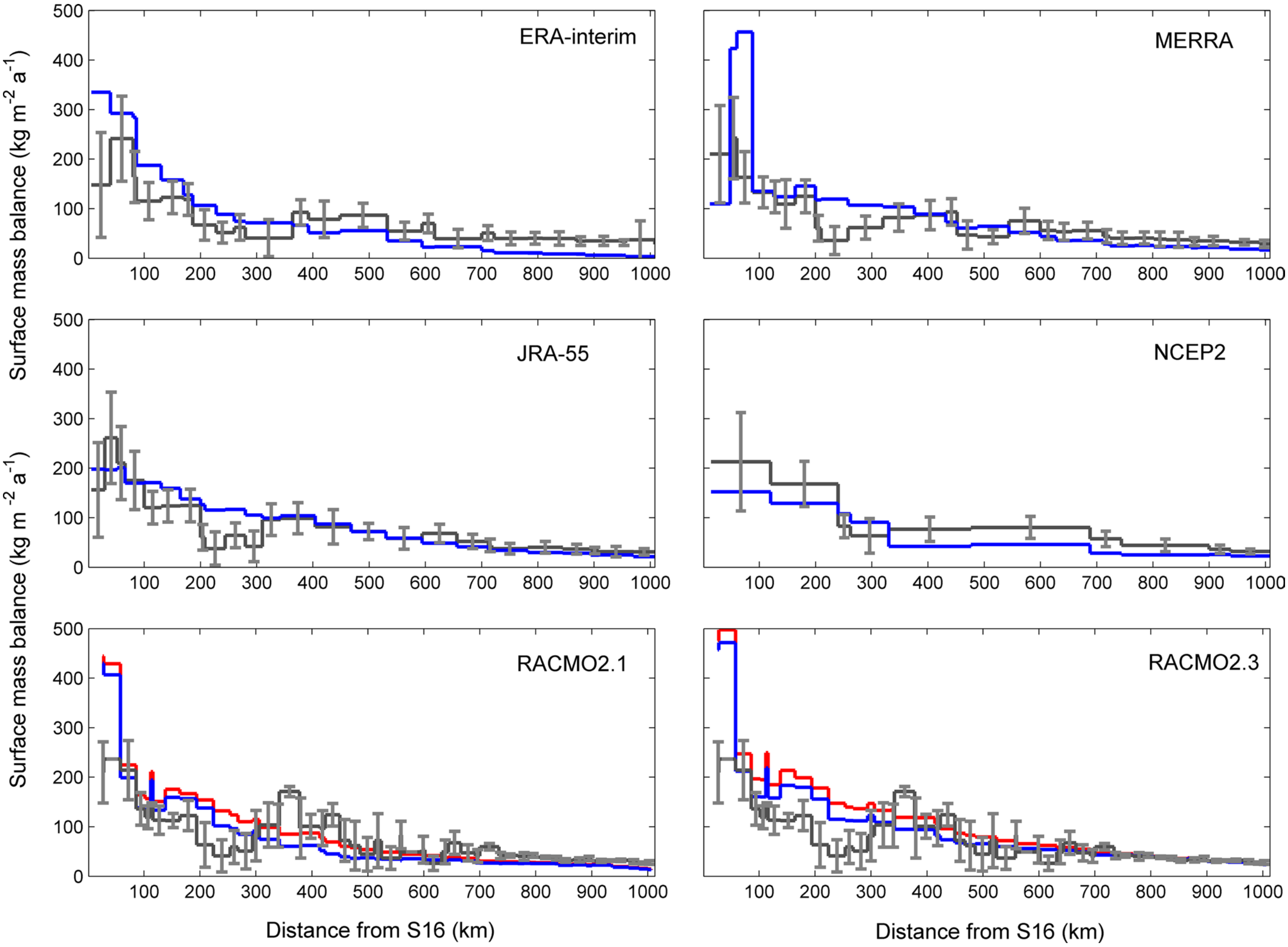

Fig. 5 Comparison of the temporally averaged surface mass balance derived from point observations and global reanalyses and regional climate model along the JARE traverse route. The averaged periods are 1979–2006 for coastal and lower katabatic regions, and 1993–2006 for upper katabatic and inland plateau regions, respectively. *Blue lines* represent the temporally averaged SMB from reanalyses and regional climate model. *Red lines* represent RACMO2.1 and RACMO2.3 SMB without wind-driven snow erosion/deposition and sublimation. *Black lines* represent the stakes SMB averaged on each model grid box

running averaged point measurements show a slight increase in 1993–2010 relative to 1993–2006 for the upper katabatic region and inland plateau region (Fig. 3). Slight increase in the inland region in the last decade also occurs in the stake line observations at the Chinese traverse from Zhong Shan Station to Dome A (Ding et al. 2011). The 20 km running mean SMB between 1975 and 1992 is slightly higher than the SMB averaged for the time span 1993–2010 for coastal region (Fig. 3). Similar pattern is also observed at other coastal regions, for example, a decrease of SMB in recent decade in the coastal region of the Chinese traverse (Ding et al. 2011).

3.3 Comparison with snow accumulation from reanalysis and regional climate model

We compare the temporally averaged SMB in a grid simulated from the four reanalyses and regional climate model with the average of measurements of all stakes that fell within the same grid (Fig. 5). To eliminate the impact of temporal variability on the multi-year averaged values of SMB, the averaged time intervals are same for observation and models (1979–2006 for coastal and lower katabatic regions; 1993–2006 for upper katabatic and inland plateau regions). All the reanalyses and regional climate model capture the large-scale decreasing pattern of SMB from S16 to Dome F, but do not reproduce the mesoscale SMB increasing trend from ~300 to ~400 km from S16. Concerning multi-year averaged SMB values for the region with <200 km distance from S16, we find that NCEP-2 simulates excessively low P–E values, leading to its overall underestimation, and large difference with point measurements occurs in MERRA, while ERA-interim, RACMO2.1 and RACMO2.3 overestimate SMB. All the atmospheric models (reanalyses and regional climate model)

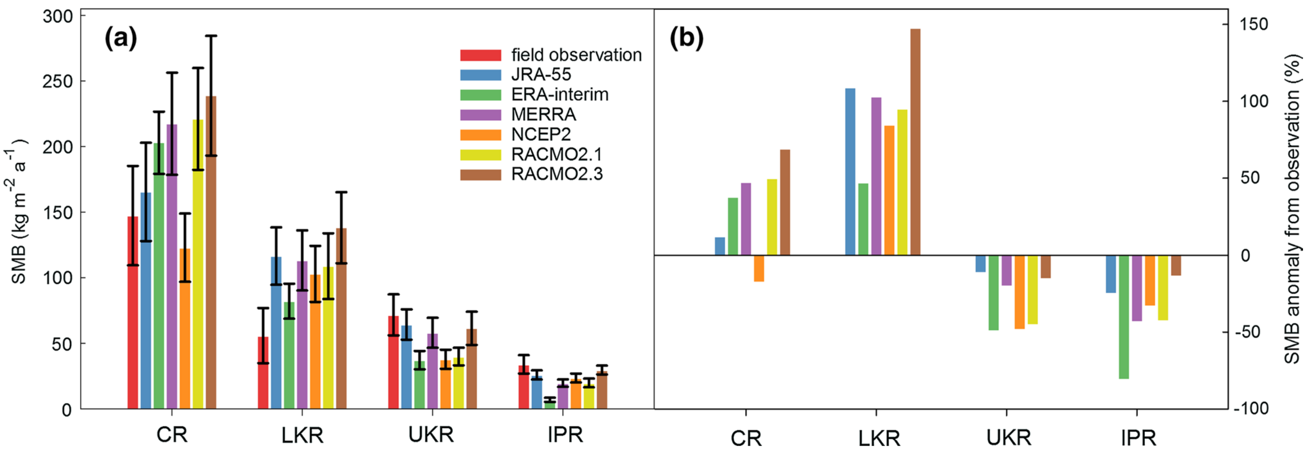

Fig. 6 Temporally-averaged SMB from field observation, reanalyses, and regional climate model (1979–2006 period) (**a**) and the percent of modelled SMB anomaly in relative to observation (**b**) for the coastal region (CR), lower katabatic region (LKR), upper katabatic region (UKR), and inland plateau region (IPR)

overestimate the SMB in about 200–300 km distance from S16. All but RACMO2.3 underestimate observed SMB in the inland region, especially the region with >700 km distance from S16. RACMO2.1 and RACMO2.3, which include snowdrift processes, show that wind-driven snow erosion–deposition and sublimation reduce the SMB in this region, but have a minor influence on the overall SMB spatial pattern (Fig. 5).

Additionally, we compare the spatially-averaged stake measurements and SMB determined by models for the different regions along the JARE traverse route divided as described above (Fig. 6). In the coastal region, NCEP2 underestimates observed SMB, while other reanalyses and the regional climate models overestimate SMB. The multi-year averaged SMB values simulated from the global reanalyses and regional climate models are higher than field observations for the lower katabatic region, but lower for the upper katabatic region. In the inland plateau region, ERA-interim underestimates observed SMB by more than 50 %, whereas the SMB simulated by RACMO2.3 shows a smaller bias (<15 %).

Figure 7 presents the inter-annual variability in spatially-averaged stake measurements and SMB simulated by global reanalyses and the regional atmospheric climate models for the four regions. The quantitative evaluation of model data performance was shown by Taylor diagrams (Fig. 8). All modelled SMB values significantly correlate with the field measurements for the coastal region, lower katabatic wind region, upper katabatic wind region ($p < 0.05$). However, in the inland plateau region, NECP2 and RACMO2.1 show no significant correlation ($p > 0.05$). ERA-interim, JRA-55 and MERRA SMB time series significantly correlates with the observed SMB in the coastal, lower katabatic, and inland plateau regions, with the correlation coefficients >0.7 ($p < 0.01$). The correlation is slightly weaker but still statistically significant in the lower katabatic region ($r < 0.6$, $p < 0.05$). Compared with RACMO2.1, RACMO2.3 has greater correlation with observation for the coastal, upper katabatic and inland plateau regions. However, its correlation is still somewhat lower than the three high-resolution reanalyses (ERA-interim, JRA-55 and MERRA).

4 Discussion

It has been recognized that cyclone trajectories, topographic relief and wind driven processes play an important role in the spatial variability of SMB (Richardson and Holmlund 1999; Van den Broeke et al. 1999; King et al. 2004; Frezzotti et al. 2005, 2007). Large-scale spatial variability of SMB in Dronning Maud Land (DML) is dominated by precipitation patterns. However, wind driven sublimation and snow redistribution can cause large differences between precipitation and SMB, especially for the coastal regions. In particular, strong wind is often associated with high-precipitation events (Fujita et al. 2011), which affects variability of SMB. The spatial pattern of SMB for this region is consistent with decreasing precipitation from the ocean to the inland plateau as shown by the Antarctic Mesoscale Prediction System (AMPS) mean annual precipitation field generated by Schlosser et al. (2008). Our results reveals a very high kilometer-scale spatial variability in SMB along the JARE traverse route, which seems to be linked to topographic features. Our data also show that this variability appears to be stationary in time (coastal and lower katabatic regions: 1975–2006; upper katabatic and inland plateau regions: 1993–2006). The dependence of SMB on elevation and continentality along this traverse route can be clearly

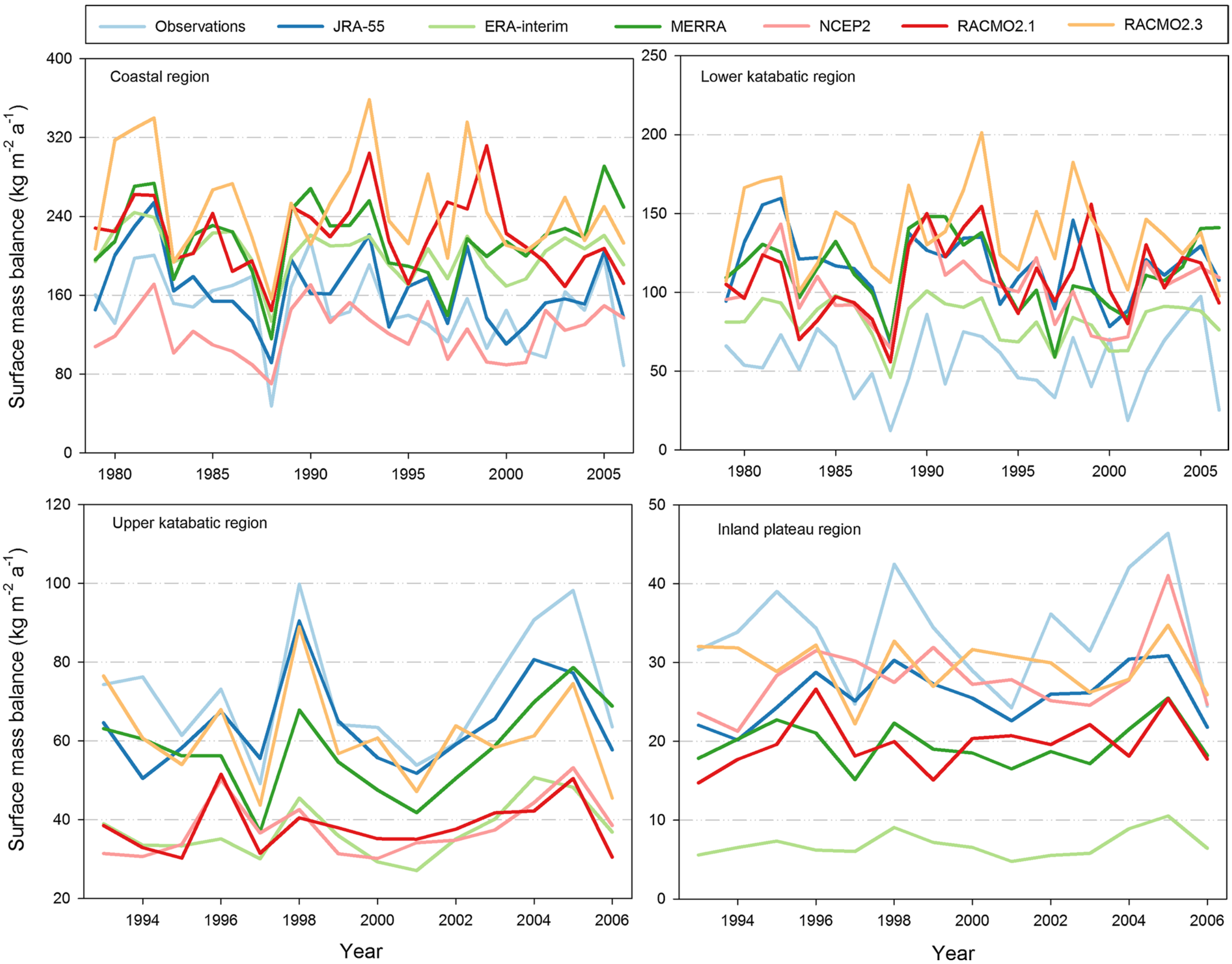

Fig. 7 The inter-annual variability in spatially-averaged stake measurements and SMB modelled by reanalyses and regional climate model for coastal region, lower katabatic region, upper katabatic region, and inland plateau region

seen in Fig. 3. To further identify spatial trends, statistical analysis was conducted to examine possible relationships between SMB and distance to S16, surface elevation, as well as surface slope which is extracted from a digital elevation model of Antarctica produced by Bamber et al. (2009). Due to robust inter-correlation between these geographic parameters (not shown), we computed the residuals resulting from the use of elevation as the predictor to remove the SMB trend induced by the elevation, and then detected the correlations between the residuals and distance to S16 and slope. Spatial variability in SMB is negatively correlated with surface elevation ($r = -0.71$, $p < 0.0001$), with a gradient of -0.04 ± 0.002 kg m^{-2} a^{-1} m^{-1}. The negative correlations are expected because of the decrease in precipitation with distance from the sea and increasing elevation (Schlosser et al. 2008). There is no significant correlation between residuals and distance to S16, probably due to high correlation between elevation and distance to S16 ($r = 0.97$, $p < 0.0001$). SMB residuals negatively correlate with the slopes with the correlation coefficient of -0.57 ($p < 0.0001$) for the lower and upper katabatic regions, which can be attributed to the impact on katabatic wind. Because strong wind can produce sastrugi and wind crust, and redistribute snow soon after it is deposited (e.g., Frezzotti et al. 2005, 2007; Urbini et al. 2008; Fujita et al. 2011), it is easily understandable that the snow accumulation is often higher on the upwind or on the leeside of a topographic obstacle.

The temporal variations and trend in SMB at a regional scale are not well determined due to different observation periods and poor spatial coverage. Our results show a negative SMB trend in the coastal region of the east DML since 1975, and a slight positive trend in the katabatic and inland plateau regions of east DML since 1993. However, these trends are statistically insignificant, which may be explained by the large inter-annual variability and the short

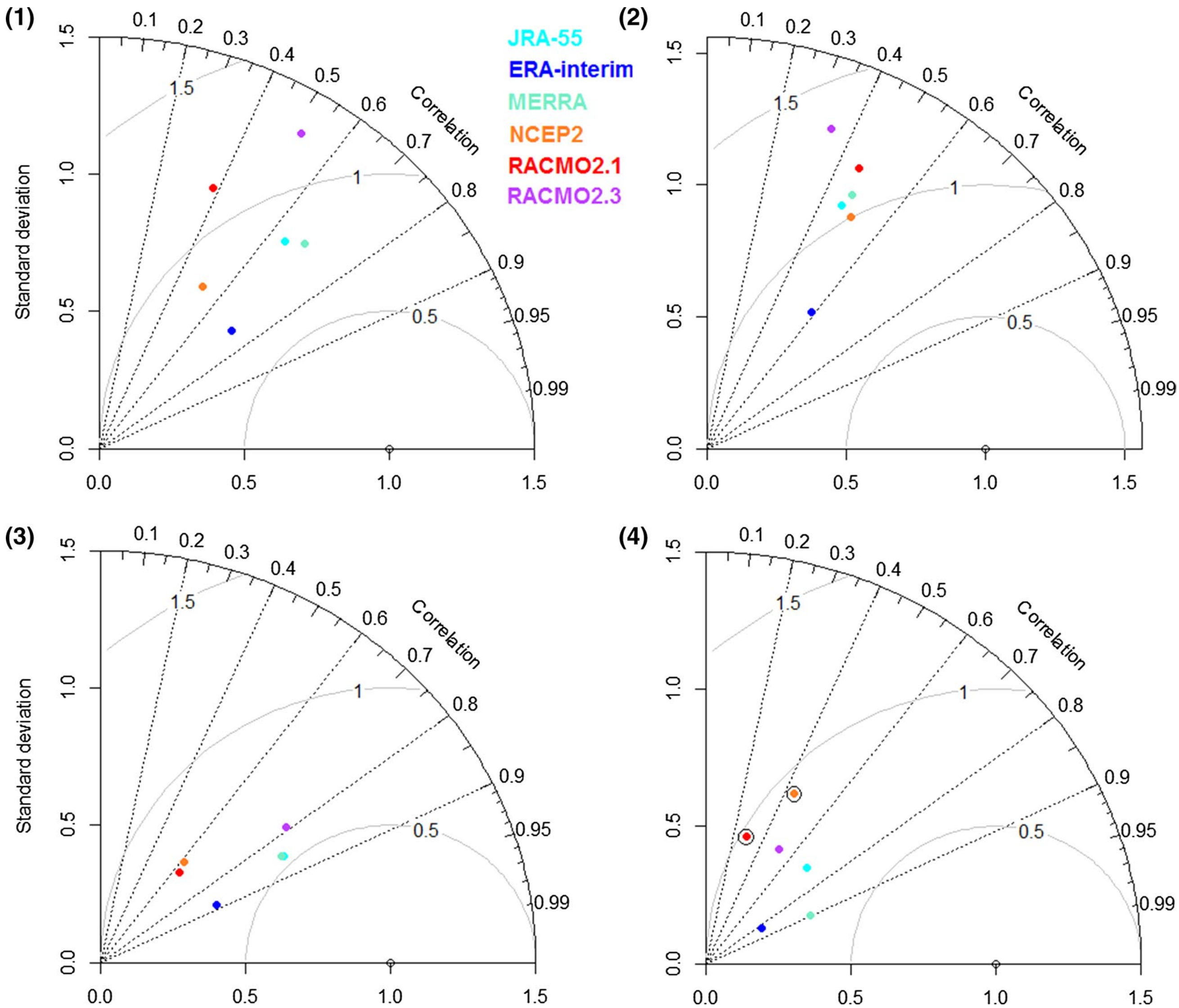

Fig. 8 Taylor diagram for the spatially-averaged correlations between field observation and modelled SMB and standard deviation for **1** coastal region, **2** lower katabatic region, **3** upper katabatic region, and **4** inland plateau region. *Point* in a *circular ring* represents <95 % significant level

time coverage of our field observations. Although firn/ice core records have the advantage to detect the long-term SMB variability and trend, based on these records, it is still difficult to determine whether regional-scale SMB in DML is increasing, decreasing, or stable in recent decades, due to the limited representation of individual cores for regional accumulation (Rotschky et al. 2007). Also, substantial basin-wide accumulation variability may contribute much to uncertainty in regional SMB estimates. For instance, by inter-comparing coastal ice core records, Kaczmarska et al. (2004) concluded a significantly negative SMB trend in the twentieth century is a regional pattern, which is constrained to coastal regions of western DML. However, in the same region, no significant temporal trend is found recorded in ice cores since the 1960s (Fernandoy et al. 2010). In contrast to a significant increasing snow accumulation in the twentieth century related to temperature variations in the dry interior of DML (Oerter et al. 2000), Anschütz et al. (2009, 2011) suggested that the largest changes probably occurred in the most recent decades with an increasing accumulation at some sites, and a decrease in other sites during the period from 1963 to present.

Figure 9 shows the comparison of surface elevation between field observations and the values used in the reanalyses and regional climate models. All the models represent the topographic variation from the coast to inland plateau well, but relatively large differences exist between field observations and models in the coastal region within 100 km S16. Moreover, NCEP2 topography differs significantly from the stake-line along the

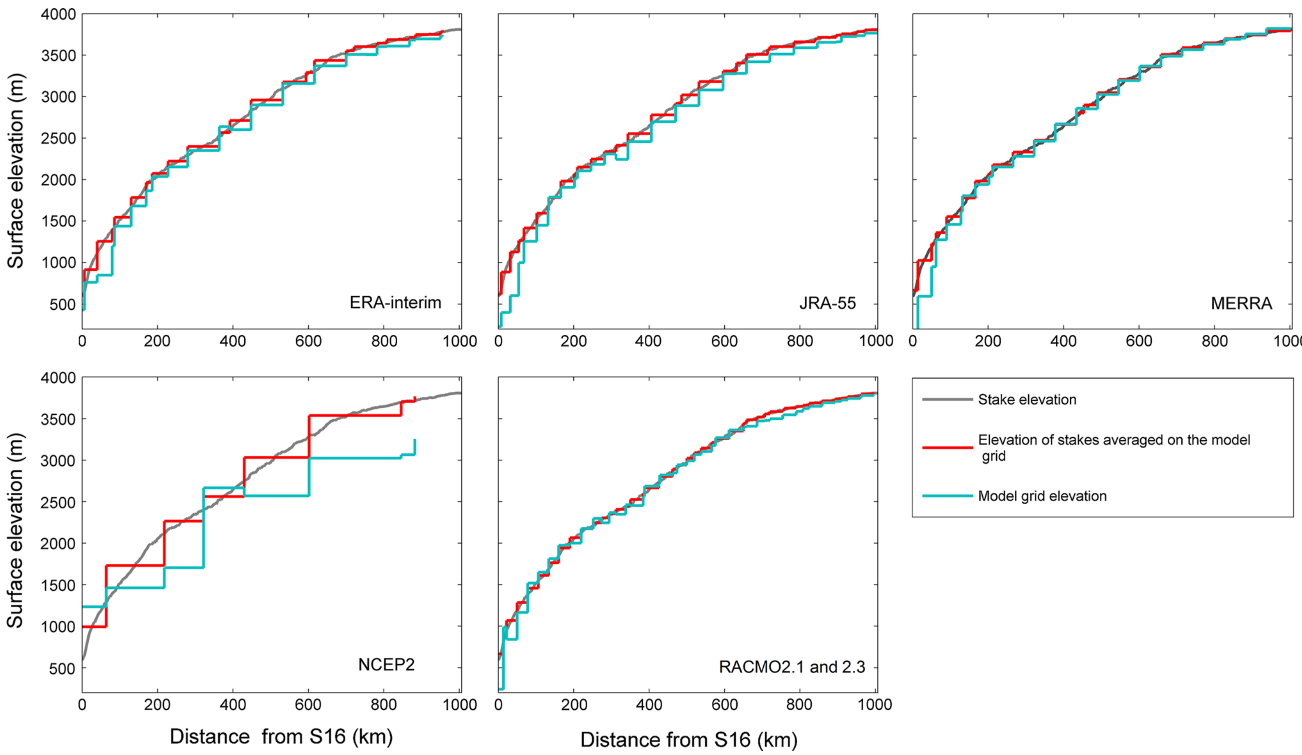

Fig. 9 Comparison between surface elevation of model grid covering the stakes and elevation of stakes over the same model grid

traverse route, due to its coarse resolution. A large part of the observed and modeled SMB discrepancies in the coastal region may be attributed to poor representation of ice sheet stake topography in the models (Agosta et al. 2012), on which many atmospheric variables such as precipitation, evaporation, energy fluxes are directly dependent. The limited skill of some models for SMB simulation also contributes to these differences. For instance, ERA-interim overestimates surface melting (Agosta et al. 2012), runoff and sublimation (Favier et al. 2013), and assumes incorrect albedo values which may result in large uncertainty in the entire surface energy balance over Antarctica (Favier et al. 2013). NCEP2's excessively low SMB for coastal region might result from the overestimation of latent heat fluxes in stable boundary layer conditions (Monaghan et al. 2006b). Bromwich et al. (2011) confirmed the dry bias in ERA-interim for the East Antarctic Plateau. However, the bias can decrease substantially if an atmospheric moisture flux budget method is used to evaluate ERA-interim precipitation minus evaporation (e.g., Bromwich and Wang 2008).

Despite the relatively good temporal correlation between MERRA based SMB and field observations in the coastal region, MERRA presents an unrealistic positive upward trend for this region (not shown), which is also confirmed by Bromwich et al. (2011). Bromwich et al. (2011) found excessively high interannual fluctuation of evaporation in relation to unrealistic total sublimation fluxes in NCEP2, which may limit its skill for the simulation of SMB.

The negative impact of wind-driven snow processes on SMB spatial variation can be clearly seen in Fig. 5. We further quantify the annual SMB and its relevant components at the four regions along the JARE traverse route based on RACMO2.3 (Fig. 10). Runoff (not shown) is zero in our study area because of the low melt rates and the subsequent refreezing of meltwater. Wind-driven erosion/deposition (ER_{ds}) shows little inter-annual variability over the four regions. Thanks to low wind velocity in the inland plateau region, and large snowfall in the coastal region, the impact of ER_{ds} on SMB is very limited (<5 % of the SMB). The magnitude of its contribution to SMB ranges from ~4 to ~8 kg m^{-2} a^{-1} for the katabatic regions. Drifting snow sublimation (SU_{ds}) is close to surface sublimation (SU_s) for the coastal region. It gets much larger than SU_s for the katabatic regions, making SU_{ds} the largest term of SMB apart from snowfall for these regions. In the inland plateau region, the magnitude of SU_s is less than 1 kg m^{-2} a^{-1}. Temporal SMB variability clearly follows to the inter-annual variation of snowfall, showing the limited impact of wind-related processes on the annual variability pattern in SMB. Reanalyses do not include a scheme for representing clear-sky precipitation, which may contribute much to SMB in the inland plateau area. They also lack some complex parameterizations of the Antarctic snowpack such

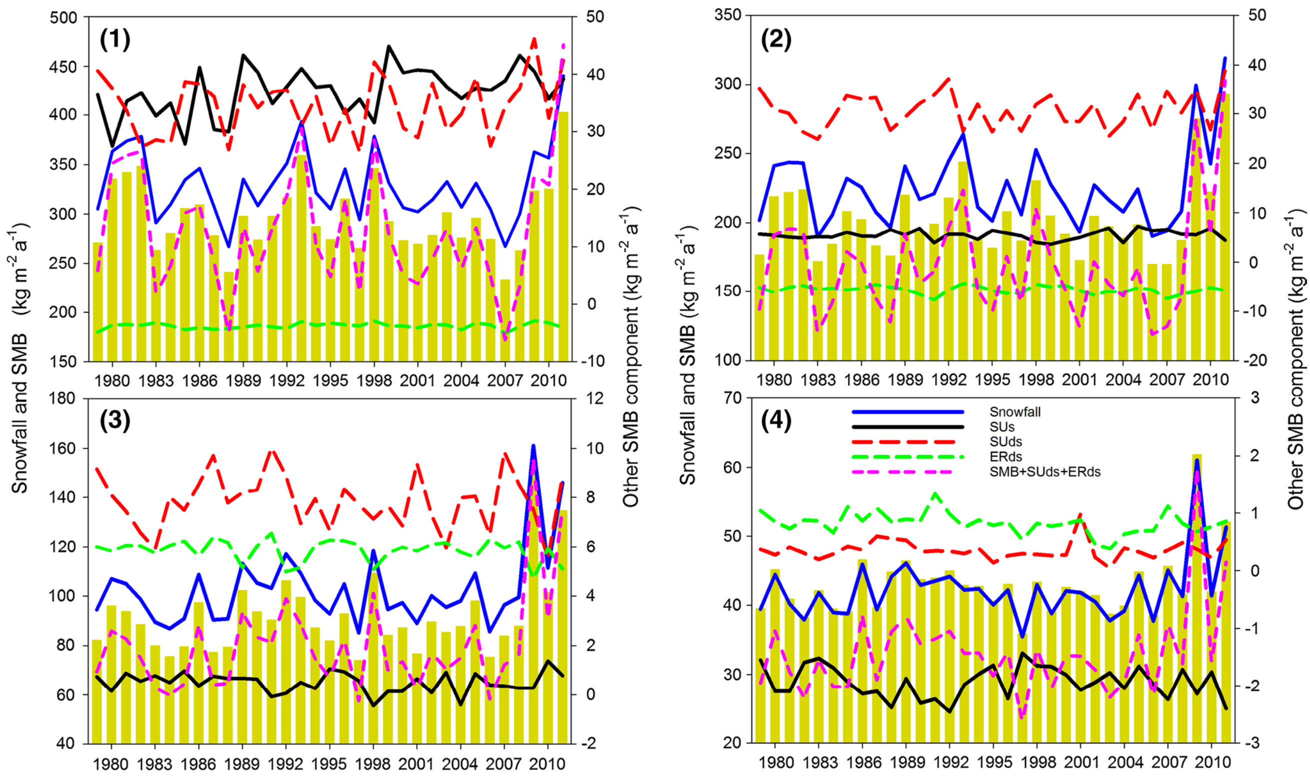

Fig. 10 Time series of SMB components over **1** coastal region, **2** lower katabatic region, **3** upper katabatic region, and **4** inland plateau region, for the period 1979–2011 from RACMO2.3. Snowfall (*blue solid line*), SMB (*bars*), and SMB without wind-driven snow erosion/deposition and sublimation (*purple dotted line*) are indicated on the *left axis*, and the other components are indicated on the *right axis*

as melt/runoff, sublimation of drifting snow particles and horizontal snow transport. Using an updated cloud microphysics scheme, RACMO2.3 substantially improves the SMB assessment for the dry inland plateau region. Blowing snow processes present a major negative effect on the SMB in the coastal and katabatic wind area, as pointed out by other studies (e.g., Frezzotti et al. 2004; Genthon et al. 2007; Lenaerts et al. 2010; Scarchilli et al. 2010). This may result in most of the inconsistency between observed SMB and SMB from reanalyses (Das et al. 2013; Scambos et al. 2012). However, SMB in the global reanalyses with simplified snow physics is still useful due to the minor influence of blowing snow processes on the spatial and inter-annual variability patterns, and the negligible contribution of meltwater runoff to the overall SMB over the grounded Antarctic Ice Sheet (Liston and Winther 2005).

5 Conclusions

SMB values derived from stake measurements and interpolated density data provide valuable information to determine its temporal and spatial variability in eastern DML. They can also be used to evaluate the variability of modeled SMB at a regional scale. Such data are of particular importance because the stake line extends over several SMB regimes from wet coastal, through the katabatic transition, to the dry interior, and annual resolution stake measurements allow the quantification of inter-annual variability in SMB. SMB averaged through 1993–2010 shows high spatial variability. The large-scale spatial variability is stationary in time, and related to distance from the coast and surface elevation. Surface slope also largely affects SMB variability in the katabatic regions. Point measurements indicate no significant SMB trends for the coastal and lower katabatic regions since mid-1970s and for the upper katabatic and inland plateau regions since mid-1990s, respectively. The lack of statistical significance in trends could be a result of the large inter-annual variability and the short time coverage of field observations, which underscores the necessity of maintaining long-term annual SMB observation and the associated logistical supports.

The large-scale spatial variability in SMB along the JARE traverse route is reasonably well represented by the four reanalyses and regional climate models. However, in terms of multi-year mean SMB, large differences between observations and simulations from all the atmospheric climate models are found in the coastal and lower katabatic region. Wind-driven snow erosion/deposition and sublimation contributes much to the inconsistency between observation and reanalysis-based SMB. These biases may be greatly reduced if the horizontal and vertical resolution of the reanalyses and atmospheric models is enhanced. Thanks to the scheme of the updated cloud microphysics, RACMO2.3 presents almost no SMB bias in the inland plateau region.

JRA-55, MERRA and ERA-interim show reasonable agreement with the annual series of the observed SMB in the coastal, upper katabatic and inland plateau regions, and moderate agreement for the lower katabatic region. Compared with the high-resolution reanalyses (ERA-interim, JRA-55 and MERRA), RACMO2.1 and RACMO2.3 show lower skills in the representation of inter-annual variability in observed SMB. This can be ascribed to the fact that no observations are assimilated in RACMO2, leaving the model interior to evolve freely. In spite of the negative contribution of wind-driven snow erosion/deposition and sublimation to SMB, the influence of these processes on the spatial and inter-annual variability pattern is minor. This is important because SMB outputs from high-resolution reanalyses which do not include wind-driven snow processes are often directly used in ice sheet SMB studies.

Acknowledgments We would like to thank National Institute of Polar Research for providing net accumulation data, Shin Sugiyama for providing snow density data, Roger J. Braithwaite and Shuangye Wu for improving the language of the paper, and two reviewers for their helpful comments and advices. The project was funded by National Key Basic Research Program of China (2013CBA01804), the Natural Science Foundation of China (41206175, 41171052), State Key Laboratory of Cryospheric Science, Cold and Arid Regions Environmental and Engineering Research Institute, CAS (SKLCS-2012-08 and SKLCS-OP-2013-01), the State Oceanic Administration (CHINARE2012-02-02), the Ministry of Education (20110091110025 and 1082020904), and China Postdoctoral Science Foundation (2014M551952).

References

Agosta C, Favier V, Genthon C, Gallée H, Krinner G, Lenaerts JTM, van den Broeke MR (2012) A 40-year accumulation dataset for Adelie Land, Antarctica and its application for model validation. Clim Dyn 38:75–86. doi:10.1007/s00382-011-1103-4

Agosta C, Favier V, Krinner G, Gallée H, Fettweis X, Genthon C (2013) High-resolution modelling of the Antarctic surface mass balance, application for the twentieth, twenty first and twenty second centuries. Clim Dyn 41:3247–3260. doi:10.1007/s00382-013-1903-9

Anschütz H, Müller K, Isaksson E, McConnell JR, Fischer H, Miller H, Albert M, Winther J-G (2009) Revisiting sites of the South Pole Queen Maud Land Traverses in East Antarctica: accumulation data from shallow firn cores. J Geophys Res. doi:10.1029/2009JD012204

Anschütz H, Sinisalo A, Isaksson E, McConnell JR, Hamran S-E, Bisiaux MM, Pasteris D, Neumann TA, Winther J-G (2011) Variation of accumulation rates over the last eight centuries on the East Antarctic Plateau derived from volcanic signals in ice cores. J Geophys Res. doi:10.1029/2011JD015753

Arthern R, Winebrenner D, Vaughan D (2006) Antarctic snow accumulation mapped using polarization of 4.3-cm wavelength emission. J Geophys Res. doi:10.1029/2004JD005667

Azuma N, Kameda T, Nakayama Y, Tanaka Y, Yoshimi H, Furukawa T, Ageta Y (1997) Glaciological data collected by the 36th Japanese Antarctic Research Expedition during 1995–1996. JARE Data Rep 223((Glaciology 26)):83

Bamber JL, Gomez-Dans JL, Griggs JA (2009) Antarctic 1 km digital elevation model (DEM) from combined ERS-1 radar and ICESat laser satellite altimetry. In: National snow and ice data center. Digital media, Boulder, Colorado USA

Barletta VR, Sørensen LSS, Forsberg R (2013) Scatter of mass changes estimates at basin scale for Greenland and Antarctica. The Cryosphere 7:1411–1432

Bosilovich MG, Chen J, Robertson FR, Adler RF (2008) Evaluation of precipitation in reanalyses. J Appl Meteorol Climatol 47:2279–2299

Bromwich DH, Wang S-H (2008) A review of the temporal and spatial variability of Arctic and Antarctic atmospheric circulations based upon ERA-40. Dyn Atmos Oceans 44:213–243

Bromwich DH, Nicolas JP, Monaghan AJ (2011) An assessment of precipitation changes over Antarctica and the Southern Ocean since 1989 in contemporary global reanalyses. J Clim 24:4189–4209. doi:10.1175/2011JCLI4074.1

Burgess EW, Forster RR, Box JE, Mosley-Thompson E, Bromwich DH, Bales RC, Smith LC (2010) A spatially calibrated model of annual accumulation rate on the Greenland Ice Sheet. J Geophys Res. doi:10.1029/2009JF001293

Conger SM, McClung DM (2009) Comparison of density cutters for snow profile observations. J Glaciol 55:163–169. doi:10.3189/002214309788609038

Das I, Bell RE, Scambos TA, Wolovick M, Creyts TT, Studinger M, Frearson N, Nicolas JP, Lenaerts JTM, van den Broeke MR (2013) Influence of persistent wind scour on the surface mass balance of Antarctica. Nat Geosci 6:367–371. doi:10.1038/ngeo1766

Davis CH, Li Y, McConnell JR, Frey MM, Hanna E (2005) Snowfall driven growth in East Antarctic ice sheet mitigates recent sea level rise. Science 308:1898–1901. doi:10.1126/science.1110662

Decker M, Brunke MA, Wang Z, Sakaguchi K, Zeng XB, Bosilovich MG (2012) Evaluation of the reanalysis products from GSFC, NCEP, and ECMWF using flux tower observations. J Clim 25:1916–1944. doi:10.1175/JCLI-D-11-00004.1

Dee DP, Uppala SM, Simmons AJ, Berrisford P, Poli P, Kobayashi S, Andrae U, Balmaseda MA, Balsamo G, Bauer P, Bechtold P, Beljaars ACM, van de Berg L, Bidlot J, Bormann N, Delsol C, Dragani R, Fuentes M, Geer AJ, Haimberger L, Healy SB, Hersbach H, Hólm EV, Isaksen L, Kållberg P, Köhler M, Matricardi M, McNally AP, Monge-Sanz BM, Morcrette J-J, Park B-K, Peubey C, de Rosnay P, Tavolato C, Thépaut J-N, Vitart F (2011) The ERA-interim reanalysis: configuration and performance of the data assimilation system. Q J R Meteorol Soc 137:553–597. doi:10.1002/qj.828

Ding M, Xiao C, Li Y, Ren J, Hou S, Jin B, Sun B (2011) Spatial variability of surface mass balance along a traverse route. J Glaciol 57:658–666

Ebita A, Kobayashi S, Ota Y, Moriya M, Kumabe R, Onogi K, Harada Y, Yasui S, Miyaoka K, Takahashi K, Kamahori H, Kobayashi C, Endo H, Soma M, Oikawa Y, Ishimizu T (2011) The Japanese 55-year Reanalysis “JRA-55”: an interim report. SOLA 7:149–152

Endo Y, Fujiwara K (1973) Characteristics of the snow cover in East Antarctica along the route of the JARE South Pole traverse and factors controlling such characteristics. JARE Sci Rep 7:1–27

Ettema J, van den Broeke MR, van Meijgaard E, van de Berg WJ, Bamber JL, Box JE, Bales RC (2009) Higher surface mass balance of the Greenland ice sheet revealed by high-resolution climate modeling. Geophys Res Lett. doi:10.1029/2009GL038110

Favier V, Agosta C, Parouty S, Durand G, Delaygue G, Gallée H, Drouet A-S, Trouvilliez A, Krinner G (2013) An updated and quality controlled surface mass balance dataset for Antarctica. The Cryosphere 7:583–597. doi:10.5194/tc-7-583-2013

Fernandoy F, Meyer H, Oerter H, Wilhelms F, Graf W, Schwander J (2010) Temporal and spatial variation of stable isotope ratios and accumulation rates in the hinterland of Neumayer station, East Antarctica. J Glaciol 56:673–687

Frezzotti M, Pourchet M, Flora O, Gandolfi S, Gay M, Urbini S, Vincent C, Becagli S, Gragnani R, Proposito M, Severi M, Traversi R, Udisti R, Fily M (2004) New estimations of precipitation and surface sublimation in East Antarctica from snow accumulation measurements. Clim Dyn 23:7–8. doi:10.1007/s00382-004-0462-5

Frezzotti M, Pourchet M, Flora O, Gandolfi S, Gay M, Urbini S, Vincent C, Becagli S, Gragnani R, Proposito M, Severi M, Traversi R, Udisti R, Fily M (2005) Spatial and temporal variability of snow accumulation in East Antarctica from traverse data. J Glaciol 51:113–124

Frezzotti M, Urbini S, Proposito M, Scarchilli C, Gandolfi S (2007) Spatial and temporal variability of surface mass balance near Talos Dome, East Antarctica. J Geophys Res 112(F02032):1–15. doi:10.1029/2006JF000638

Fujita S, Holmlund P, Andersson I, Brown I, Enomoto H, Fujii Y, Fujita K, Fukui K, Furukawa T, Hansson M, Hara K, Hoshina Y, Igarashi M, Iizuka Y, Imura S, Ingvander S, Karlin T, Motoyama H, Nakazawa F, Oerter H, Sjöberg LE, Sugiyama S, Surdyk S, Ström J, Uemura R, Wilhelms F (2011) Spatial and temporal variability of snow accumulation rate on the East Antarctic ice divide between Dome Fuji and EPICA DML. The Cryosphere 5:1057–1081

Fujiwara K, Endo Y (1971) Preliminary report of glaciological studies. JARE Sci Rep Spec Issue 2:68–109

Furukawa T, Kamiyama K, Maeno H (1996) Snow surface features along the traverse route from the coast to Dome Fuji Station, Queen Maud Land, Antarctica. Proc NIPR Symp Polar Meteorol Glaciol 10:13–24

Gallée H, Trouvilliez A, Agosta C, Genthon C, Favier V, Naaim-Bouvet F (2013) Transport of snow by the wind: a comparison between observations in Adélie Land, Antarctica, and simulations made with the regional climate model MAR, Bound.-Lay. Meteorology 146:133–147

Genthon C, Lardeux P, Krinner G (2007) The surface accumulation and ablation of a coastal blue-ice area near Cap Prudhomme, Adélie Land, Antarctica. J Glaciol 53:635–645. doi:10.3189/002214307784409333

Giovinetto M, Zwally H (2000) Spatial distribution of net surface mass accumulation on the Antarctic ice sheet. Ann Glaciol 31:171–178

GSI (2007) 50 Years of Antarctic Research Expeditions by the Geographical Survey Institute Planning Department, Geodetic Department, and Topographic Department. Bull GSI 54

Hanna E, Huybrechts P, Cappelen J, Steffen K, Bales RC, Burgess E, McConnell JR, Steffensen JP, Van den Broeke M, Wake L, Bigg G, Griffiths M, Savas D (2011) Greenland Ice Sheet surface mass balance 1870 to 2010 based on twentieth century reanalysis, and links with global climate forcing. J Geophys Res. doi:10.1029/2011JD016387

Helsen MM, van den Broeke MR, van de Wal RSW, van de Berg WJ, van Meijgaard E, Davis CH, Li YH, Goodwin I (2008) Elevation changes in Antarctica mainly determined by accumulation variability. Science 320:1626–1629. doi:10.1126/science.1153894

Kaczmarska M, Isaksson E, Karlöf L, Winther J-G, Konhler J, Godtliebsen F, Olsen LR, Hofstede CM, van den Broeke MR, van de Wal RSW, Gundestrup N (2004) Accumulation variability derived from an ice core from coastal Dronning Maud Land, Antarctica. Ann Glaciol 39:339–345

Kameda T, Motoyama H, Fujita S, Takahashi S (2008) Temporal and spatial variability of surface mass balance at Dome Fuji, East Antarctica, by the stake method from 1995 to 2006. J Glaciol 54:107–116

King JC, Anderson PS, Vaughan DG, Mann GW, Mobbs SD, Vosper SB (2004) Wind-borne redistribution of snow across an Antarctic ice rise. J Geophys Res. doi:10.1029/2003JD004361

Lenaerts JTM, Van den Broeke MR (2012) Modeling drift snow in Antarctica with a regional climate model. 2. Results. J Geophys Res. doi:10.1029/2010JD015419

Lenaerts JTM, van den Broeke MR, Déry SJ, König-Langlo G, Ettema J, Munneke PK (2010) Modelling snowdrift sublimation on an Antarctic ice shelf. The Cryosphere 4:179–190. doi:10.5194/tc-4-179-2010

Lenaerts JTM, Van den Broeke MR, Van de Berg WJ, Meijgaard EV, Munneke PK (2012a) A new, high-resolution surface mass balance map of Antarctica (1979–2010) based on regional atmospheric climate modeling. Geophys Res Lett. doi:10.1029/2011GL050713

Lenaerts JTM, Van den Broeke MR, Dery SJ, van Meijgaard E, van de Berg WJ, Palm SP, Sanz Rodrigo J (2012b) Modeling drifting snow in Antarctica with a regional climate model: 1. Methods and model evaluation. J Geophys Res. doi:10.1029/2011JD016145

Ligtenberg SRM, Kuipers Munneke P, van den Broeke MR (2014) Present and future variations in Antarctic firn air content. The Cryosphere 8:1711–1723. doi:10.5194/tc-8-1711-2014

Liston GE, Winther J-G (2005) Antarctic surface and subsurface snow and ice melt fluxes. J Clim 18:1469–1481

Medley B, Joughin I, Das SB, Steig EJ, Conway H, Gogineni S, Criscitiello AS, McConnell JR, Smith BE, van den Broeke MR, Lenaerts JTM, Bromwich DH, Nicolas JP (2013) Airborne-radar and ice-core observations of annual snow accumulation over Thwaites Glacier, West Antarctica confirm the spatiotemporal variability of global and regional atmospheric models. Geophys Res Lett 40:3649–3654. doi:10.1002/grl.50706

Monaghan AJ, Bromwich DH, Fogt RL, Wang S, Mayewski PA, Dixon DA, Ekaykin A, Frezzotti M, Goodwin I, Isaksson E, Kaspari SD, Morgan VI, Oerter H, Van Ommen TD, Van der Veen CJ, Wen J (2006a) Insignificant change in Antarctic snowfall since the international geophysical year. Science 313:827–831. doi:10.1126/science.1128243

Monaghan AJ, Bromwich DH, Wang S-H (2006b) Recent trends in Antarctic snow accumulation from Polar MM5 simulations. Philos Trans R Soc A364:1683–1708

Moore P, King MA (2005) Antarctic ice mass balance estimates from GRACE: tidal aliasing effects. J Geophys Res. doi:10.1029/2007JF000871

Motoyama H, Fujii Y (1999) Glaciological data collected by the 38th Japanese Antarctic Research Expedition during 1997–1998. JARE Data Rep 28:1–74

Motoyama H, Furukawa T, Nishio F (2008) Study of ice flow observations in Shirase drainage basin and around Dome Fuji area, East Antarctica, by differential GPS method. Antarct Rec 52:216–231 (in Japanese with English summary)

Naruse R (1975) Density and hardness of snow in Mizuho Plateau in 1969–1970. JARE Data Rep 27((Glaciology 2)):180–186

Oerter H, Wilhelms F, Jung-Rothenhäusler F, Göktas F, Miller H, Graf W, Sommer S (2000) Accumulation rates in Dronning Maud Land, Antarctica, as revealed by dielectric-profiling measurements of shallow firn cores. Ann Glaciol 30:27–34

Ohmae H (1984) Density of surface snow cover along routes S, H and Z. JARE Data Rep 94:62–63

Onogi K, Tsutsui J, Koide H, Sakamoto M, Kobayashi S, Hatsushika H, Matsumoto T, Yamazaki N, Kamahori H, Takahashi K, Kadokura S, Wada K, Kato K, Oyama R, Ose T, Manoji N, Taira R (2007) The JRA-25 reanalysis. J Meteorol Soc Jpn 85:369–432

Richardson C, Holmlund P (1999) Spatial variability at shallow snow-layer depths in central Dronning Maud Land, East Antarctica. Ann Glaciol 29:10–16

Rienecker MM, Suarez MJ, Gelaro R, Todling R, Bacmeister J, Liu E, Bosilovich MG, Schubert SD, Takacs L, Kim G-K, Bloom S, Chen J, Collins D, Conaty A, da Silva A, Gu W, Joiner J, Koster RD, Lucchesi R, Molod A, Owens T, Pawson S, Pegion P, Redder CR, Reichle R, Robertson FR, Ruddick AG, Sienkiewicz M, Woollen J (2011) MERRA: NASA's modern-era retrospective analysis for research and applications. J Clim 24:3624–3648. doi:10.1175/JCLI-D-11-00015.1

Rignot E, Velicogna I, van den Broeke MR, Monaghan A, Lenaerts JTM (2011) Acceleration of the contribution of the Greenland and Antarctic ice sheets to sea level rise. Geophys Res Lett. doi:10.1029/2011GL046583

Rotschky G, Holmlund P, Isaksson E, Mulvaney R, Oerter H, Van den Broeke MR, Winther JG (2007) A new surface accumulation map for western Dronning Maud Land, Antarctica, from interpolation of point measurements. J Glaciol 53:385–398

Sasgen I, Konrad H, Ivins ER, Van den Broeke MR, Bamber JL, Martinec Z, Klemann V (2013) Antarctic ice-mass balance 2003 to 2012: regional reanalysis of GRACE satellite gravimetry measurements with improved estimate of glacial-isostatic adjustment based on GPS uplift rates. The Cryosphere 7:1499–1512. doi:10.5194/tc-7-1499-2013

Satow K, Watanabe O, Shoji H, Motoyama H (1999) The relationship among accumulation rate, stable isotope ratio and surface temperature on the plateau of east Dronning Maud Land, Antarctica. Polar Meteorol Glaciol 13:43–52

Scambos TA, Frezzotti M, Haran T, Lenaerts JTM, Bohlander J, Van Den Broeke MR, Jezek K, Long D, Urbini S, Farness K, Neumann T, Albert M, Winther J-G (2012) Extent of low-accumulation 'wind glaze' areas on the East Antarctic plateau: implications for continental ice mass balance. J Glaciol 58:633–647. doi:10.3189/2012JoG11J232

Scarchilli C, Frezzotti M, Grigioni P, Silvestri LD, Agnoletto L, Dolci S (2010) Extraordinary blowing snow transport events in East Antarctica. Clim Dyn 34:1195–1206

Schlosser E, Duda MG, Powers JG, Manning KW (2008) Precipitation regime of Dronning Maud Land, Antarctica, derived from Antarctic Mesoscale Prediction System (AMPS) archive data. J Geophys Res. doi:10.1029/2008JD009968

Shepherd A, Ivins ER, Geruo A, Barletta VR, Bentley MJ, Bettadpur S, Briggs KH, Bromwich DH, Forsberg R, M Horwath, Galin N, Jacobs S, Joughin I, King MA, Lenaerts JT, Li J, Ligtenberg SR, Luckman A, Luthcke SB, McMillan M, Meister R, Milne G, Mouginot J, Muir A, Nicolas JP, Paden J, Payne AJ, Pritchard H, Rignot E, Rott H, Sørensen LS, Scambos TA, Scheuchl B, Schrama EJ, Smith B, Sundal AV, van Angelen JH, van de Berg WJ, van den Broeke MR, Vaughan DG, Velicogna I, Wahr J, Whitehouse PL, Wingham DJ, Yi D, Young D, Zwally H (2012) A reconciled estimate of ice-sheet mass balance. Science 338:1183–1189. doi:10.1126/science.1228102

Simmons A, Uppala S, Dee D, Kobayashi S (2009) ERA-interim: new ECMWF reanalysis products from 1989 onwards. ECMWF Newsletter, No. 110, ECMWF, Reading, United Kingdom, 25–35. http://www.ecmwf.int/publications/newsletters/pdf/110_rev.pdf

Sinisalo A, Anschütz H, Aasen AT, Langley K, von Deschwanden A, Kohler J, Matsuoka K, Hamran S-E, Øyan M-J, Schlosser E, Hagen JO, Nøst OA, Isaksson E (2013) Surface mass balance on Fimbul ice shelf, East Antarctica: comparison of field measurements and large-scale studies. J Geophys Res (Atmos) 118:11625–11635. doi:10.1002/jgrd.50875

Sugiyama S, Enomoto H, Fujita S, Fukui K, Nakazawa F, Holmlund P, Surdyk S (2012) Snow density along the route traversed by the Japanese–Swedish Antarctic Expedition 2007/08. J Glaciol 58:529–539

Takahashi S, Ageta Y, Fujii Y, Watanabe O (1994) Surface mass balance in east Dronning Maud Land, Antarctica, observed by Japanese Antarctic Research Expeditions. J Glaciol 20:242–248

Urbini S, Frezzotti M, Gandolfi S, Vincent C, Scarchilli C, Vittuari L, Fily M (2008) Historical behaviour of Dome C and Talos Dome (East Antarctica) as investigated by snow accumulation and ice velocity measurements. Glob Planet Change 60:576–588

Van de Berg WJ, Van den Broeke MR, Reijmer C, Van Meijgaard E (2006) Reassessment of the Antarctic surface mass balance using calibrated output of a regional atmospheric climate model. J Geophys Res. doi:10.1029/2005JD006495

Van den Broeke MR, Michael R, Jan-Gunnar W, Elisabeth I, Jean Francis P, Lars K, Trond E, Louk C (1999) Climate variables along a traverse line in Dronning Maud Land, East Antarctica. J Glaciol 45:295–302

Van Wessem JM, Reijmer CH, Morlighem M, Mouginot J, Rignot E, Medley B, Joughin I, Wouters B, Depoorter MA, Bamber JL, Lenaerts JTM, van de Berg WJ, van den Broeke MR, van Meijgaard E (2014) Improved representation of East Antarctic surface mass balance in a regional atmospheric climate model. J Glaciol 60:761–770. doi:10.3189/2014JoG14J051

Vaughan D, Bamber J, Giovinetto M, Russell J, Cooper A (1999) Reassessment of net surface mass balance in Antarctica. J Clim 45:933–946

Velicogna I (2009) Increasing rates of ice mass loss from the Greenland and Antarctic ice sheets revealed by GRACE. Geophys Res Lett. doi:10.1029/2009GL040222

Watanabe O (1975) Density and hardness of snow in Mizuho Plateau-West Enderby Land in 1970–1971. JARE Data Rep 27((Glaciol 2)):187–235

Watanabe O (1978) Distribution of surface features of snow cover in Mizuho Plateau. Mem Natl Inst Polar Res (Spec Issue) 7:44–62

Wingham DJ, Shepherd A, Muir A, Marshall GJ (2006) Mass balance of the Antarctic ice sheet. Philos Trans R Soc A364:1627–1635

Zwally HJ, Giovinetto MB (2011) Overview and assessment of Antarctic Ice-Sheet mass balance estimates: 1992–2009. Surv Geophys 32:351–376